Solar Organic Rankine Cycle coupled with Reverse Osmosis and mebrane distillation towards minimizing brine discharge

Erika Ntavou[1], Marina Micari[2], Dimitris Manolakos[1], George Kosmadakis[3] and Chrysanthos Golonis[1]

[1] Agricultural University of Athens, Athens (Greece)

[2] Deutsches Zentrum für Luft- und Raumfahrt (German Aerospace Center), Stuttgart (Germany)

[3] Ricreation IKE, Technological Park "Lefkippos", Athens (Greece)

Abstract

The current research work is focused on the investigation, optimization and identification of key design parameters of a solar-Organic Rankine Cycle (ORC) power generation system coupled with Reverse Osmosis (RO) and Membrane Distillation (MD) desalination units for fresh water production. The core idea is to feed RO and MD units by exploiting both electricity generated by the ORC and the heat dissipated in the ORC condenser respectively. Electricity comes from the direct conversion of heat to power through ORC and is used to drive the system pumps, while heat for MD corresponds to that dissipated during condensation process (heat rejection of the power cycle). By combining RO with MD an increased water recovery ratio from both desalination processes can be achieved, resulting into reduction of the environmentally harmful brine. Further exploitation of the high concentrate is possible to extract sodium chloride crystals. The proposed system can be flexibly combined with other thermal sources (e.g. excess heat from industrial processes) and it is applicable for feed water treatment of different salinities (brackish, seawater etc.). Vacuum tube solar collectors operating at temperature in the order of 130 ^{o}C have been considered in the calculations. The condensation temperature where heat is supplied to MD is in the order of 90 ^{o}C, Some 90 kWth of heat are rejected in the full load operation, while net power generation from the ORC is about 3 kW with a thermal efficiency slightly above 3.5 %.

Keywords: solar Organic Rankine Cycle, RO desalination, Membrane Distillation, Zero Brine Discharge

1. Introduction

The rapid recent increase in population has created the necessity of intensive water consumption in the human environment. Water desalination appears to be an appropriate technology to cover this increased need. In recent decades, water production has largely shifted to the reverse osmosis (RO) technology, because of its lower energy consumption compared to other desalination technologies (i.e. thermal). The lower consumption has been achieved through the application of energy recovery systems and thanks to the evolution of membranes technology. However, desalination remains an energy-cost intensive water treatment process with serious environmental impacts. In addition to the contribution of desalination to CO_2 emissions, significant environmental burden is incurred due to the rejection of the high concentration of saline solution (brine) as a by-product of the process resulting in soil, aquifer and marine ecosystems pollution. Any effort to mitigate CO_2 and brine disposal environmental effects is of significance towards improving desalination environmental profile and constitutes a complex techno-economical challenge.

Normally, the brine from seawater desalination units using open ocean intakes has the same physical characteristics as the seawater feeding the system since no chemicals are added in the pre-treatment of the RO system, thus increase or decrease in salinity would not result in a severe environmental impact. However, dense concentrate disposal may lead to increased stratification reducing vertical mixing, thus reducing the dissolved oxygen level in water or at the bottom of the ocean in the area of the discharge, which may result in ecological implications (Mickley 2006). Some key environmental issues and considerations linked to the concentrate disposal to surface waters are the increase of salinity over the tolerance barrier of the marine flora and fauna and the discharge of nutrients that trigger a change in the area of the discharge, the ion-imbalance toxicity caused by the mixture of incompatible composition of the desalination plant concentrate and receiving waters and the disturbance in seabed from outfall installation (Voutchkov 2011).

Therefore, a serious concern is growing around the environmental impact of desalination systems and especially the

Selection and/or peer review under responsibility of Scientific Committee
doi:10.18086/eurosun.2020.12.06 Available at http://proceedings.ises.org

impact on marine life close to the plant intakes and outfalls. Several countries are already discussing strict regulations on seawater desalination concentrate discharge, including zero discharge regulations. As Navar et al. (2019) point out, the interest of policy makers and the industry in understanding the technical and economic implications of zero brine discharge regulations is growing.

At the same time, the CO_2 footprint of the RO plants operation when using conventional energy sources is high. Heihsel et al. (2019) studied the 95% of Australia's RO plants' operation for a decade (assuming that all are using fossil fuels) and pointed out that in both construction and operation, the role of the electricity sector is critical for carbon emissions, each contributing in 69% during the zenith of the construction phase and 96% during the operating phase to the entire emissions, with a total estimation for 2015 at 1193 kt CO_2e.

Recently, much research has been done on seawater RO zero liquid discharge desalination. Tufa et al. (2015) have investigated an innovative approach combining Direct Contact Membrane Distillation (DCMD) and Reverse Electrodialysis (RE), for water and energy production from RO concentrate, thus implementing the concept of low energy and Near-Zero Liquid Discharge in seawater desalination, proving that the DCMD operated on 1 M NaCl RO brine fed at 40–50 °C resulted in a volume reduction factor up to 83.6%. Davis (2006), studied a zero liquid discharge ZLD process for seawater reverse osmosis using electrodialysis (ED) to reduce the salinity of the concentrate from the RO, so that the low salinity reject stream can be recycled to the RO to improve freshwater while producing salable sodium chloride (NaCl), magnesium hydroxide ($Mg(OH)_2$), and bromine (Br_2) from the brine. The results of this study indicated that the use of electrodialysis can reduce the potential detrimental impact of discharging the reject stream to the ocean and if fully implemented, the process could produce high-purity NaCl, Mg $(OH)_2$, Br_2, and mixed dry salts with zero liquid discharge. Al-Obaidani et al. (2015) studied the integration of conventional pressure-driven membranes with the innovative units of membrane contactors such as membrane distillation (MD)/crystallization for concentrate treatment and zero liquid discharge achievement and revealed that the pressure-driven membrane operations were very sensitive to the feed concentration and the cost of electricity consumption, while MD processes were not.

However, the tackling of the high energy and cost of the RO process requires a much more thorough study according to the state of the art. The technology of the Organic Rankine Cycle (ORC) used to convert low grade heat (less than 150 ^{o}C) to electricity, with high conversion efficiency and maturity, in combination to a RO unit has recently started to be investigated. Nevertheless, as the state-of-the-art indicates, there is no research combining the ORC and RO technology towards a near zero liquid discharge.

The current research aims to study, optimize and identify key design parameters of a solar-ORC system combined with RO and MD to maximize the water recovery ratio of the saline feed water. Thus, by exploiting the renewable solar energy, a high value natural resource, water, is produced with a limited environmental footprint for both CO_2 and brine.

2. System description

The current work is the evolution of an already theoretical-experimental work realized within the frame of the research project "Two-stage RO-Rankine", partly funded by the Greek General Secretary of Research and Technology (GSRT), where an autonomous two-stage solar ORC system for RO desalination was investigated. Ntavou et al. (2016 and 2017) have developed and experimentally evaluated a small-scale two-stage ORC engine operating at low temperature, electrically feeding a multi-skid reverse osmosis unit operating at fluctuating power input (see fig. 1). More specifically, a two-stage solar ORC operating with 100 kW_{th} heat input and at around 100-130 °C produced a maximum of ~10 kW of electricity from both stages ($P_{ex,1}$ +$P_{ex,2}$), which operated three identical seawater RO desalination units connected in parallel, of a maximum production of 2,1m^3/h. The RO units were operating with a recovery of 38% and the integrated system was tested for several operation points in different heat input, thus different power input for the RO. The results revealed an efficient operation but the "free" concentrate discharge of the system is still an issue to take into account. Therefore, the system has been further improved by including MD technology that can offer more distilled water by exploiting the heat dissipating from ORC.

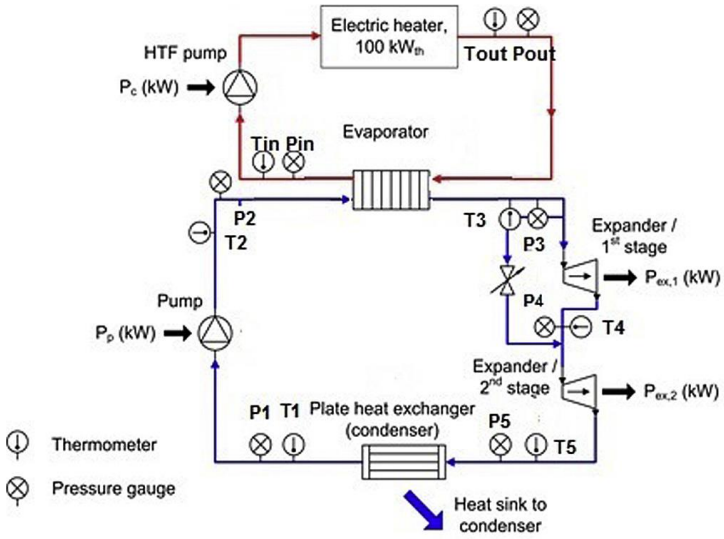

Fig. 1: The two-stage ORC unit

The investigated integrated system layout is depicted in Figure 2 below and is briefly described as follows. Heat is produced from a ~100kW$_{th}$ solar collectors' field. Vacuum tube solar collectors are chosen for this task due to their favorable efficiency in elevated ranges of operation temperature (130-150 ^{o}C). This heat is supplied to the evaporator of the ORC engine and leads to the evaporation of the working fluid (refrigerant) at a slightly lower temperature. The produced superheated vapor at the outlet of the evaporator is driven to the ORC expander (volumetric machine, scroll type in this case), producing electricity that is supplied to ORC feed pump, RO and MD pumps. The RO unit is fed by seawater and produces two water streams: the low salinity (permeate) water and the rejected high salinity (brine) solution which is then directed to the MD unit in order to recover additional fresh water. Thus, in this way, the entire process water recovery ratio can be enhanced.

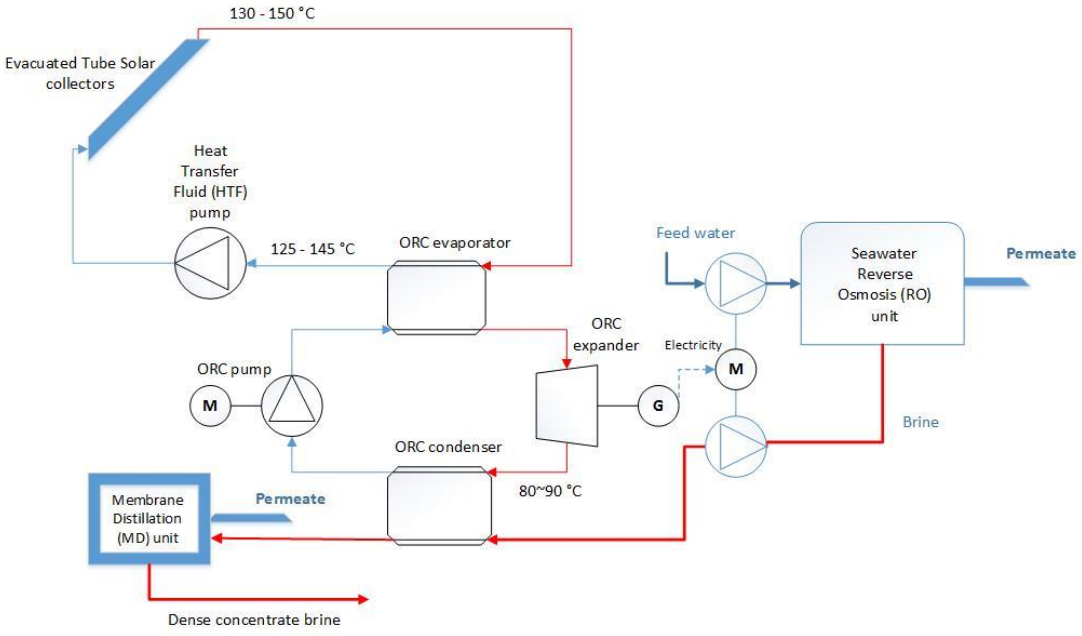

Fig. 2: The integrated solar ORC for RO-MD desalination

The RO unit is equipped with an energy recovery system in order to bring down specific electricity consumption, in the order of ~4-5 kWh/m^3. The heat required for the MD operation is extracted by the condensation process of the ORC at an appropriate temperature range of 80-90°C. This allows the MD unit to operate with hot temperatures between 70 and 80°C, which ensure a high driving force for the vapor flux through the membrane when the cold temperature is around 20°C.

3. System's simulation

Different modelling tools are developed to simulate and optimize the process and technologies involved. An EES steady state model is implemented to simulate the solar collectors and ORC technologies and validated with experimental results, derived from the Two-Stage-Solar ORC. RO is simulated using ROSA software and MD with a multi-hierarchy model, implemented in Python and derived from the work of Micari et al. (2020).

3.1 The solar collectors

For the case under investigation, the Thermomax DF-100, 3m^2 collector's model is considered, with glycol as working fluid. In Table 1, the specific characteristcs of this collector are presented.

Tab. 1: Solar collectors field characteristics

Product	Thermomax collector DF-100 3m^2
Absorber area, A_{abs} (m^2)	3.020
η_o (-)	0.832
a_{c1} (W/m^{2}K)	1.14
a_{c2} (W/m^{2}K^2)	0.0144
Inclination (^{o})	35
No of collectors, N_c	50
Outlet temperature, $T_{c,out}$ (^{o}C)	133
Inlet temperature, $T_{c,in}$ (^{o}C)	128

To investigate the performance of the vacuum tube solar collector, the definition of the incidence angle modifier (IAM) is crucial to calculate the collector's efficiency and heat generation with more accuracy. In the specification sheet of the specific model, K_b (θ_long), K_b (θ_trans) and K_d (θ) are provided (see table 2).

Tab. 2: Thermomax DF-100 3m^2 IAM

	0°	10°	20°	30°	40°	50°	60°
K_b (θ_trans)	1.00	1.01	1.02	1.03	1.01	0.94	0.80
K_b (θ_long)	1.00	1.00	0.99	0.98	0.96	0.92	0.86
K_d (θ)	0.88						

Accordingly, the collector output is given by the following equation:

$$\dot{q}_{col} = \eta_0 \cdot (K_b(\theta) \cdot G_{bT} + K_d(\theta) \cdot G_d) - a_{c1} \cdot (T_m - T_e) - a_{c2} \cdot (T_m - T_e)^2 \quad [\text{W/m}^2] \quad \text{(eq. 1)}$$

and the total heat produced by the collectors' $\dot{Q}_{col}$array is:

$$\dot{Q}_{col} = N_c \cdot A_{abs} \cdot \frac{\dot{q}_{col}}{1000} \quad [\text{kW}] \quad \text{(eq. 2)}$$

The efficiency η_{col} of the collectors' array can be expressed as:

$$\eta_{\text{col}} = \frac{\dot{q}_{\text{col}}}{G_{\text{tot}}} \cdot 100 \quad [\%] \quad \text{(eq. 3)}$$

G_{tot} [W/m^2] is the total solar irradiance on the collectors' surface.

The mass flow rate of the glycol in the collectors' circuit can then be calculated as:

$$\dot{m}_{\text{col}} = \frac{\dot{Q}_{\text{col}}}{c_{\text{p}} \cdot (T_{c,out} - T_{c,in})} \quad [\text{kg/s}] \quad \text{(eq. 4)}$$

3.2 The ORC engine

As already mentioned, a two-stage ORC system with two scroll expanders in series has already been investigated and the results have been already published. In two-stage operation, however, the organic fluid having expanded further in the second expander, has used more of the available kWth and its saturation temperature drops to around 30°C at the condenser. However, this temperature is very low for the efficient MD operation. Thus, for the ORC only the high-pressure stage operation is considered. Consequently, the new system configuration lacks the power produced by the low-pressure stage on one hand, but the condensation temperature raises to the order of 90 ºC that is ideal for the MD efficient operation.

The ORC uses R-245fa as working fluid due to its favorable properties in the selected operation temperature. The cycle is presented at the design conditions in the P- h chart of Fig. 5, which shows the power consumed by the pump (W_p), the power produced from the expander (W_{exp}), the evaporation heat (Q_{ev}) provided by the collectors and the condensation rejected heat (Q_{cond}) which is the driving force for the MD operation. The cycle is considered to operate mostly at constant evaporation-condensation temperature. This can be realized to a considerable extent by regulating appropriately the mass flow rate of the ORC making use of a pump inverter.

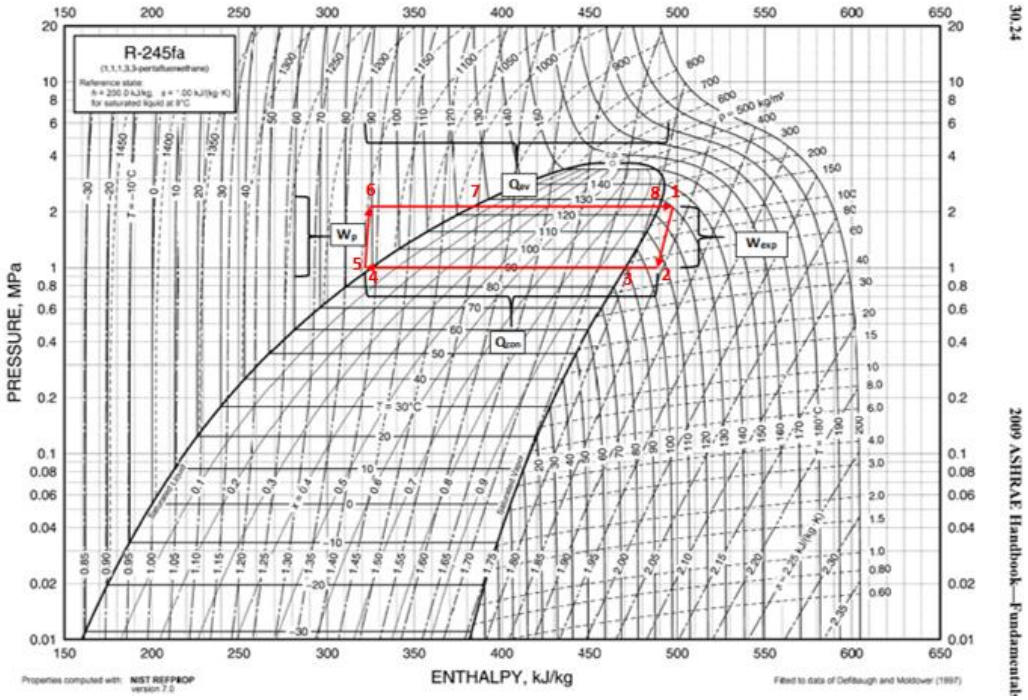

Fig. 3: The ORC cycle on R-245fa P-h chart at design conditions

The states of the thermodynamic cycle of Fig. 5 are illustrated in Table 3.

Tab. 3: States of the cycle

State	S1 (SH vapor)	S2 (SH vapor)	S3 (Sat vapor)	S4 (Sat. liquid)
Temperature (ºC|)	129.8	102.7	89.61	89.61
State	S5 (SC liquid)	S6 (SC liquid)	S7 (Sat liquid)	S8 (Sat. vapor)
Temperature (ºC|)	86.61	87.72	126.8	126.8

SC: sub-cooling SH: Super-heating

In order to evaluate the expander's operation, a polynomial has been derived from the experimental data. More specifically, the isentropic efficiency of the expander is expressed with the following polynomial as a function of pressure ratio (PR) and filling factor (FF) and it is generated by the experimental data derived during testing of the high-pressure expander:

$$\eta_{\text{exp}} = a_0 + a_1 \cdot PR + a_2 \cdot PR^2 + a_3 \cdot FF + a_4 \cdot PR \cdot FF + a_5 \cdot PR \cdot FF^2 + a_6 \cdot PR^2 \cdot FF + a_7 \cdot PR^2 \cdot FF^2 \quad [-] \qquad \text{(eq. 5)}$$

To formulate it, 166 experimental data were processed with a convergence coefficient of R^2=98.26 %. The expression of the isentropic efficiency is valid for PR values in the range between 1.5 and 3.0, and for FF from 1.16 to 9.6. Table 4, summarizes the values of polynomial's factors from a_0 to a_7.

Tab. 4: Expander's isentropic efficiency polynomial factor

a_0	a_1	a_2	a_3
-4.68763263	5.30488508	-1.27035570	1.10352750
a_4	a_5	a_6	a_7
-1.35711599	0.0345269529	0.339770213	-0.0122545150

The power $\dot{W}_{exp}$ generated by the expander is:

$$\dot{W}_{exp} = \eta_{\text{exp}} \cdot \dot{m}_{\text{p}} \cdot (h_1 - h_{2,\text{is}}) \quad \text{[kW]} \quad \text{(eq. 6)}$$

h_1 and $h_{2,\text{is}}$ [kJ/kg] represent the enthalpies at the inlet and the isentropic outlet of the expander.

Concerining the power absorbed by the ORC feed pump $\dot{W}_{pump}$, it is defined as:

$$\dot{W}_{pump} = \frac{\dot{m}_{\text{p}} \cdot (h_{6,is} - h_5)}{\eta_{pump}} \quad \text{[kW]} \quad \text{(eq. 7)}$$

where η_{pump} is the isentropic efficiecny of the ORC feed pump and $h_{6,is}, h_5$[kJ/kg] are the isentropic enthalpy at the outlet and the enthalpy at the inlet of the pump.

The mass flow rate in the ORC engine circuit $\dot{m}_{\text{p}}$ can be calculated by assuming that the evaporator losses are negligible and thus, the total heat gain of the collectors is transfereed to the ORC engine ($\dot{Q}_{orc,ev} = \dot{Q}_{col}$):

$$\dot{m}_{\text{p}} = \frac{\dot{Q}_{\text{orc,ev}}}{h_1 - h_6} \quad \text{[kg/s]} \quad \text{(eq. 8)}$$

The net power produced by the ORC is given by the eqauation below:

$$\dot{W}_{net} = \dot{W}_{exp} - \dot{W}_{pump} \quad \text{[kW]} \quad \text{(eq. 9)}$$

Finally the reject heat $\dot{Q}_{rej}$ that is to drive the MD unit is expressed as:

$$\dot{Q}_{rej} = \dot{m}_{\text{p}} \cdot (h_2 - h_5) \quad \text{[kW]} \quad \text{(eq. 10)}$$

To have a more realistic approach for the real heat supply tot the MD the above expreassion results are combined with the exparimetal values at the same conditions. This comparison indicates a further 10% reduction in the calculateed values, reflecting to the heat losses in the ORC circuit.

4. Results and discussion

Several simulation tests have been conducted for the solar collectors' operation. In Figure 4, the solar irradiance on the inclined collectors' surface and the heat gain are presented for a representative summer day (2nd of July 2019). For that, real meteorological data provided by the National Observatory of Athens were used. The whole system behavior is analyzed for his day.

4.1 Solar collectors

As shown in Fig.4, the solar collectors produce heat for ten hours (from 6:00 to 16:00 UTC), reaching a pick of around 85 kWth. This heat is provided to the ORC engine. The solar irradiance shows a maximum value of the order of 1000 W/m^2

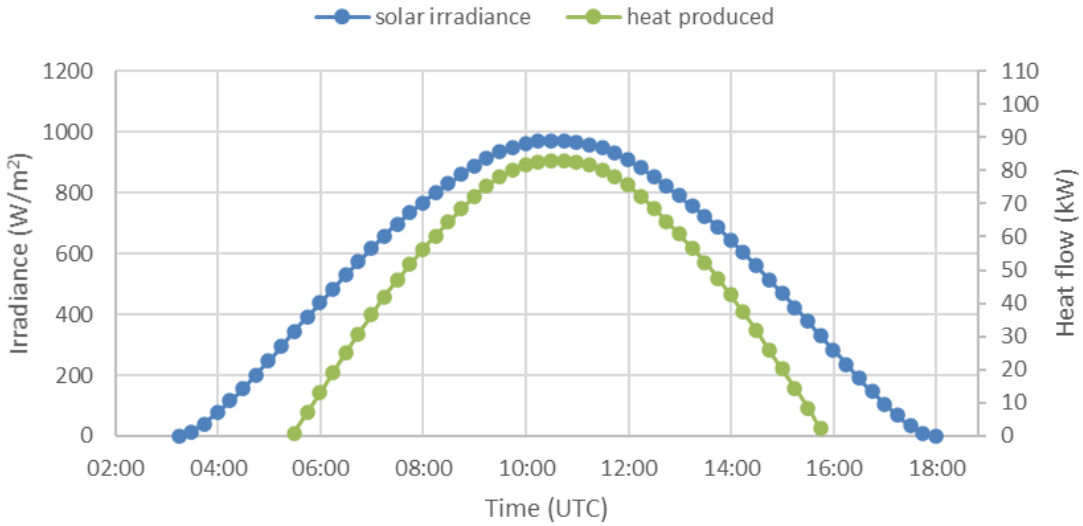

Fig. 4: Solar collectors' heat gain and solar irradiance variation

The collectors' efficiency is presented in Fig. 5, where the glycol mass flow rate in the collectors' circuit is also shown. The maximum efficiency of the solar collectors' is about 55 % and the glycol mass flow rate in the order of 4 kg/s (~14.5 m^3/h) that also constitutes the nominal flow rate of the collectors' circuit pump.

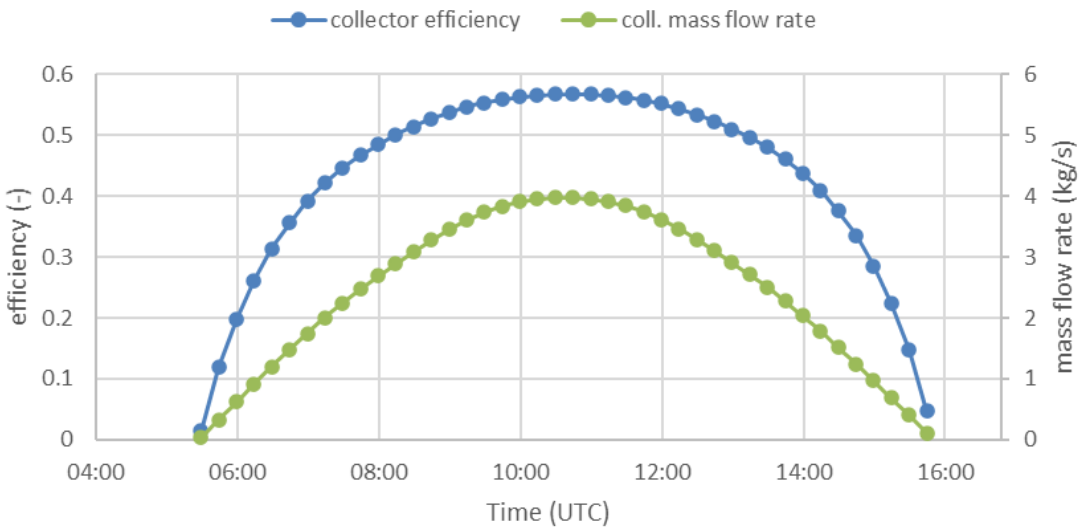

Fig. 5: Solar collectors' efficiency and mass flow rate

4.2 ORC engine

For the ORC cycle of Fig. 3, the pressure ratio is 2.2 (Inlet pressure 22 bar, Outlet pressure 10 bar). The filling factor depends on the mass flow rate of the working fluid, meaning that it is finally a function of the rotation speed. At the design point the filling factor is 1.16 corresponding to a rotational speed of the expander of ~3200 RPM (the working fluid mass flow rate is about 0.5 kg/s in this condition). In the calculations, a feed pump of isentropic efficieny equal to 70% is considered. The isenrropic efficiency of the expander is around 58 % while the thermal efficiecny of the cycle is 3.7 %. Figure 6 shows the variation of the power produced by the expander, the power absorbed by the pump and the net power for the simulation day.

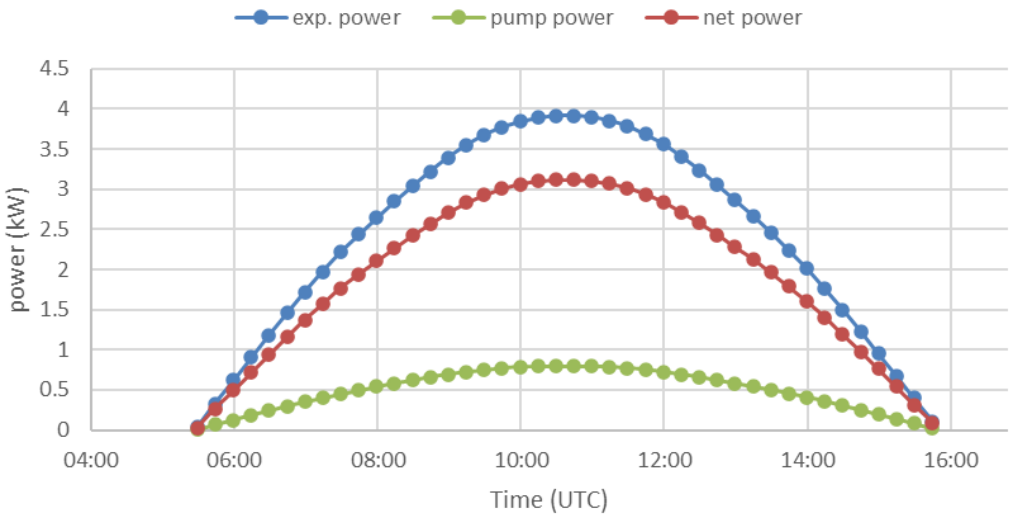

Fig. 6: Expander's, pump's and net ORC power production

While the expander provides a maximum power in the order of 4 kW, the pump absorbs around 0.8 kW and finally the net power avaliable does not exceed the 3.3 kW.

The heat supply to the evaporator, the heat rejected by the condenser and the variation of the mass flow rate of the working fluid are presented in Fig. 7. The heat rejected is supplied to the MD unit. According to Table 3, this heat is mostly available at 89.61 ºC since this is the latent heat released by condensation for the phase change process. De-superheating represents no more that 10 % of the global condensation heat.

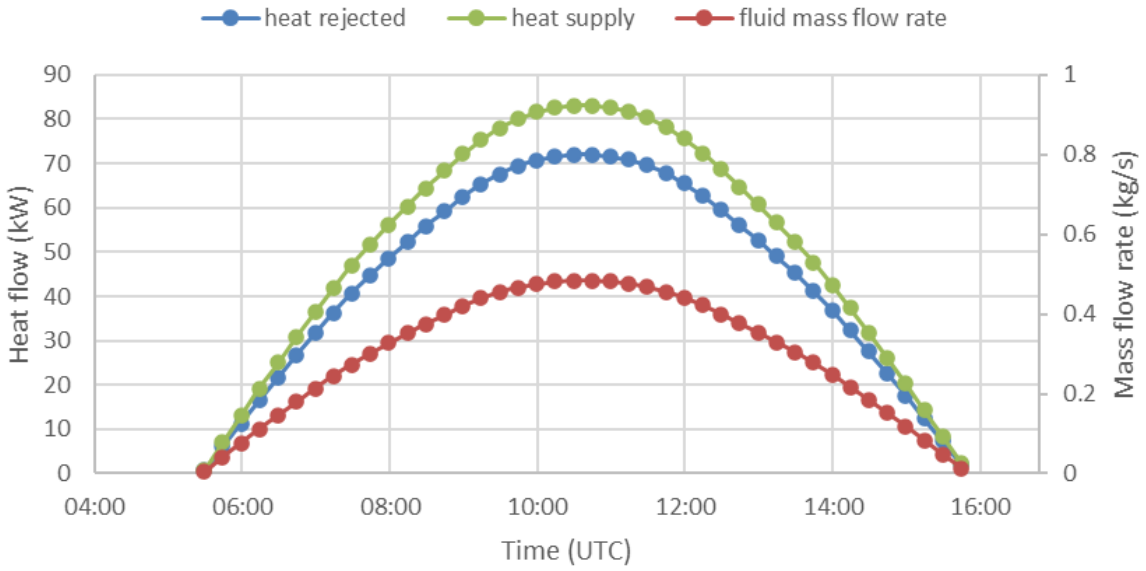

Fig. 7: ORC heat supply, heat rejected and mass flow rate variation

Thus, the MD is designed to operate with heat flow in the order of 70 kWth at a temperature of ~85 ºC (considering the temperature difference in the condenser sides).

4.3 The RO unit

The simulation of the RO unit is based on the experimental testing of the three identical sub-units used in the previous project of Ntavou et al. (2016 and 2017). The three units are now replaced by one RO unit, the recovery is 35% and the specific energy consumption 4.3 kWh/m^3, a value that has been experimentally extracted. In Fig. 8, the fresh water and brine generated by the RO for all the power input range from the ORC are presented.

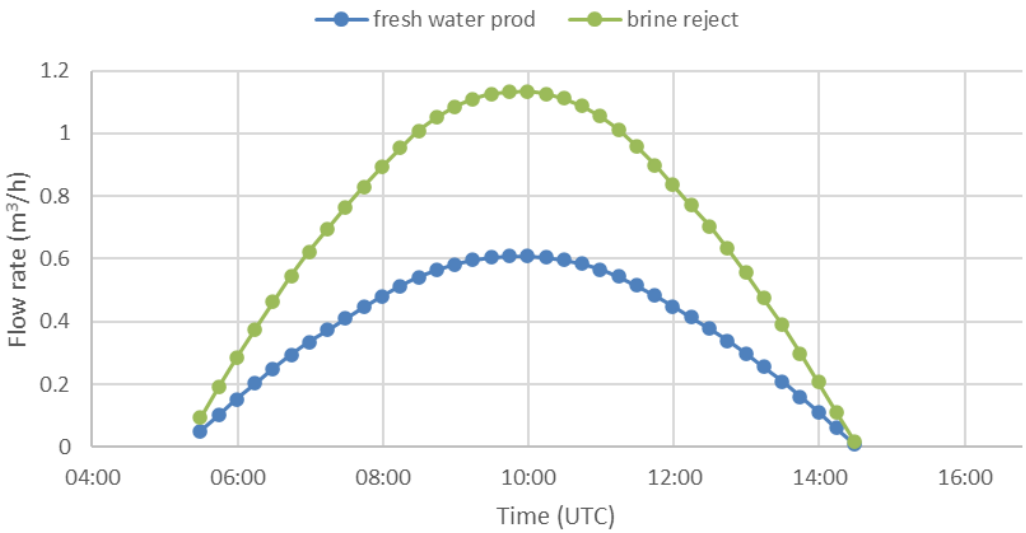

Fig. 8 Fresh water and brine production of the RO unit

The maximum brine flow rate produced by the RO reaches a value of around 1.2 m^3/h. The total concentration of the brine stream is around 65.000 ppm as resulted from the ROSA simulation tool and the expander outlet temperature around 89°C.

4.4 The MD unit

The MD unit is designed based on the brine flow rate generated by the RO unit. This consists of a number of modules in series, each given by 6 membrane sheets with length of 3 m wounded together in a spiral wound arrangement. Each module is designed for a feed flow rate of 1.5 m^3/h, thus, for the present system, only one branch of MD modules in series is required. The feed channel is kept at a temperature of 80ºC, whereas the permeate channel is at ambient temperature (20ºC). The system, with 4 modules in series, is designed to achieve a maximum recovery of around 20%, corresponding to a concentration of the rejected brine of 80,000 ppm. The specific thermal consumption is 700 kWh/m^3, thus, the permeate production varies depending on the heat availability. In Fig. 9, the permeate production of the MD is presented for the specific day of operation of the integrated system.

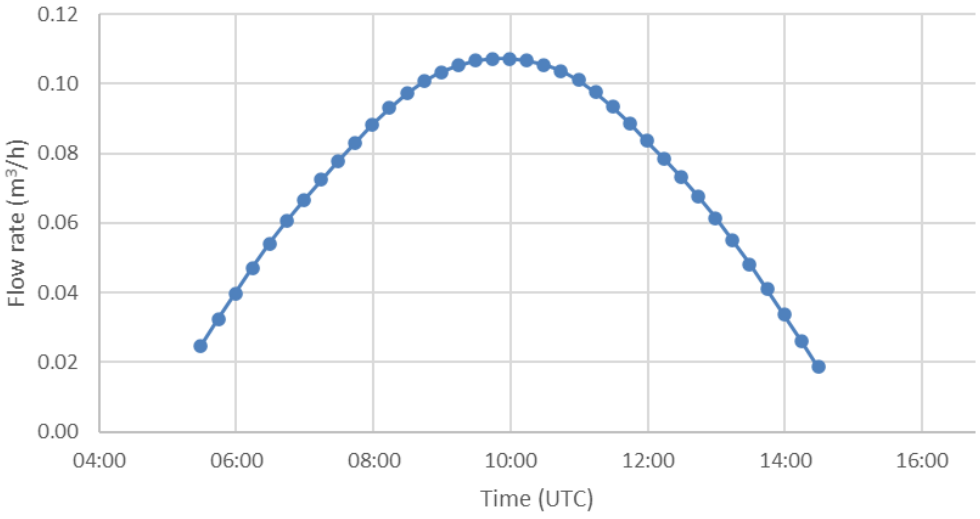

Fig. 9: Contribution on the permeate production from the MD unit

As resulted from the MD operation, the maximum contribution of the MD to the permeate production is around 110L/h. That means that the contribution of the MD system to the RO operation is low, however important. Nevertheless, the goal towards the NZL discharge seems to not be met under the specific conditions and design of the system. The reason for this is that the MD module needs high amounts of available heat in order to operate efficiently, whereas the heat given by the ORC condensation was able to cover only a limited increase in concentration. In addition, in order to produce thermal energy at a temperature suitable to MD operation, only the first expander of the ORC engine was considered, and this led to a power production lower than the one deriving

from the initially designed engine, thus to lower fresh water and brine production in the RO unit. However, the system presented in this work is in principle able to meet the target of the NZL discharge and its energy efficiency can be improved by designing a suitable ORC for the energy supply and by including additional steady heat sources to achieve higher recovery in the MD unit.

5. Conclusions

In the current work, an integrated autonomous ORC system combined to a RO unit and an MD unit for the brine treatment has been evaluated to minimize brine discharge. The MD unit exploited the rejected heat of the ORC condensation. According to the results of the simulations based on experimental data, the system provided 3.2 kW of net electricity and 70 kW of thermal energy at 85ºC when the heat supply rate is in the order of 85 kW (i.e. ORC thermal efficiency of 3.7 %). With the electricity provided by the ORC, the RO unit produced a maximum of 0.6 m^3/h permeate when fed by 1.8 m^3/h seawater (feed concentration: 40,000 ppm, water recovery ratio: 35%). Then, the brine (1.20 m^3/h) was fed to the MD, whose operation was driven by the thermal energy supplied by the ORC. In these operating conditions, the MD was able to recover around 0.11 m^3/h of additional distillate. The overall system allowed for recovering 0.7 m^3/h from a feed flow of 1.7 m^3/h (considering a specific heat consumption for MD ~700 kWth/m^3).

As resulted from the current investigation, the MD contribution to the RO fresh water production is low, however important. This is because the heat provided by the ORC condensation was not enough to assure high productivity in the MD unit which is a very energy intensive process. However, this shortcoming is counterbalanced to some extent from the very high quality of the distilled water produced. Moreover, the consideration of only one ORC expander's operation in order to meet the necessary outlet conditions for the MD operation, led to a lower power production from the ORC, thus a lower production from the RO. The intermittent availability of solar energy also imposes operation in part-load. Future work will concern the employment of an independent heat supply to the MD in order to treat the brine more efficiently and to achieve higher fresh water recovery. In this case zero brine discharge could be achieved.

6. Acknowledgments

This research is co-financed by Greece and the European Union (European Social Fund- ESF) through the Operational Programme «Human Resources Development, Education and Lifelong Learning» in the context of the project "Reinforcement of Postdoctoral Researchers – 2nd Cycle" (MIS-5033021), implemented by the State Scholarships Foundation (IKY).

The present work has been based in the previous project of the authors, conducted within the framework of the "*Twostage RO-Rankine*" project No. 09SYN-32-982, partly funded by the Greek General Secretary of Research and Technology (GSRT). The research teams would also like to thank their partners for their work conducted within this project.

Ευρωπαϊκή Ένωση
European Social Fund
Operational Programme
Human Resources Development, Education and Lifelong Learning
Co-financed by Greece and the European Union
ΕΣΠΑ 2014-2020

7. References

Al-Obaidani S., Al-Abri M., Al-Rawahi N., (2015). Achieving the Zero-Liquid-Discharge Target Using the Integrated Membrane System for Seawater Desalination, in: An Overview: Desalination, Environment and Marine Outfall Systems (pp.53-72)

Davis A.T., 2006. Zero Discharge Seawater Desalination: Integrating the Production of Freshwater, Salt, Magnesium, and Bromine. Desalination and Water Purification Research and Development Program Report No. 111 https://www.usbr.gov/research/dwpr/reportpdfs/report111.pdf

Heihsel M., Lenzen M., Malik A., Geschke A., 2019. The carbon footprint of desalination: An input-output analysis of seawater reverse osmosis desalination in Australia for 2005–2015. Desalination, 454, 71-81.

Micari M., Moser M., Cipollina A., Tamburini A., Micale G., and V. Bertsch. 2020. Towards the Implementation of Circular Economy in the Water Softening Industry: A Technical, Economic and Environmental Analysis. Journal of Cleaner Production. Article number 12029.

Mickley M.C., 2006. Membrane Concentrate Disposal: Practices and Regulation, Desalination and Water Purification Research and Development Program Report N. 123 (Second Edition), U.S. Department of Interior, Bureau of Reclamation, 128.

Nayar G.K., Fernandes J., McGovern K.R., Al-Anzi S.B., Lienhard H.J., 2019. Cost and energy needs of RO-ED-crystallizer systems for zero brine discharge seawater desalination. Desalination, 457, 115-132.

Ntavou, E., Kosmadakis, G., Manolakos, D., Papadakis, G., Papantonis, D., 2016. Experimental evaluation of a multi-skid reverse osmosis unit operating at fluctuating power input. Desalination, 398, 77-86.

Ntavou, E., Kosmadakis, G., Manolakos, D., Papadakis, G., Papantonis, D., 2017. Experimental testing of a small-scale two stage Organic Rankine Cycle engine operating at low temperature. Energy, 141, 869-879.

Voutchkov N., 2011. Overview of seawater concentrate disposal alternatives. Desalination, 273, 205-219.

https://water.custhelp.com/app/answers/detail/a_id/7835/related/1 (01/29/2020)